

Solvent-free Fluids Based on Rhombohedral Nanoparticles of Calcium Carbonate

Qi Li,^{†,‡} Lijie Dong,^{†,‡} Wei Deng,[†] Qingming Zhu,[†] Yun Liu,[†] and Chuanxi Xiong^{*,†,‡}

School of Materials Science and Engineering, and State Key Laboratory of Advanced Technology for Materials Synthesis and Processing, Wuhan University of Technology, Wuhan 430070, People's Republic of China

Received March 20, 2009; E-mail: cxx@live.whut.edu.cn

Calcium carbonate (CaCO₃) nanoparticles (NPs) are extensively used as the inorganic part of organic–inorganic nanocomposites because of their dimensional stability, high rigidity, fine thermal properties, and low cost. Due to the high surface energy, CaCO₃ NPs are easy to agglomerate,^{1,2} which makes them difficult to process or even deteriorate the mechanical properties of their composites. The lack of functionalities is another obstacle to the widespread application of CaCO₃ NPs. Fabricating a soft organic shell onto a nanostructure surface through covalent bonding to produce a sort of solvent-free nanofluid (nanoparticle suspension) has been a proven strategy to enhance the processability of NPs and impart novel functionalities to NPs.^{3–6} To date, various nanostructures have been functionalized with this approach, and all behave in a liquid-like manner after the functionalization.^{7–14} Nevertheless, solvent-free fluids based on NPs of inorganic salt have yet to be reported, and one of the possible reasons may be the insufficiency of a surface hydroxyl group for the covalent bonding of coupling agents.

It is reported that the aqueous slurry of CaCO₃ NPs has a basic pH of 9.4,¹⁵ and under ambient conditions, CaCO₃ has OH groups on the surface.¹⁶ The pH value was adjusted to 10–12 in our synthesis procedure so that more OH groups would be attached to the incompletely coordinated calcium ions on the surface, and a basic pH of ~10.5 was proven to be favorable in promoting the condensation of OH groups on other inorganic particles surfaces.¹⁷ By investigating the X-ray photoelectron spectroscopy (XPS) of C1s and Ca2p core levels from CaCO₃ NPs both before and after adjusting the pH value (Figure S1), we found surface differences in the two cases. Under an adjusted pH value, we successfully synthesized the solvent-free fluids based on CaCO₃ NPs in a facile and user-friendly method. Since we can only obtain a solid-like product based on CaCO₃ NPs without adjusting the pH value, it can be concluded that the pH adjustment is effectual.

Four significant characteristics of the functionalized CaCO₃ NPs can be listed here: (i) the fluidity derived from the soft organic shell will be of great value for processability, manipulation, and ease of dispersion; (ii) the CaCO₃ fluids are intrinsically conductive, which is a new functionality for CaCO₃ NPs; (iii) the rhombohedral CaCO₃ NPs possess a larger surface area than spherical NPs with the same volume, which results in a higher organic content in the organic–inorganic core/shell system, and once orderly accumulating is achieved, they will arrange more closely than spherical NPs, which may be favorable to the mechanical properties of their composites; (iv) the nontoxicity of the CaCO₃ core and zero vapor pressure of the organic shell make this system totally nonpolluting. Remarkably, we not only extended the range of solvent-free fluids but also obtained some high-resolution transmission electron micros-

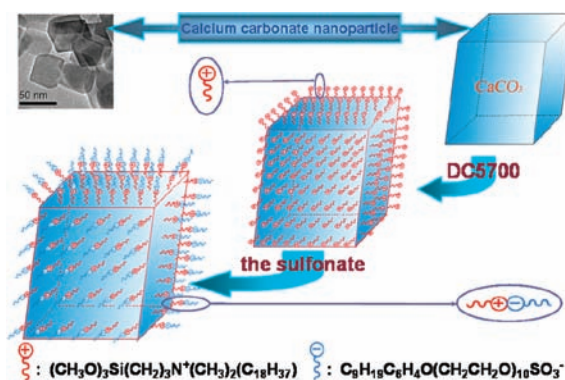


Figure 1. Scheme of the preparation of CaCO₃ sulfonate nanosalt and TEM image of original CaCO₃ NPs (top left).

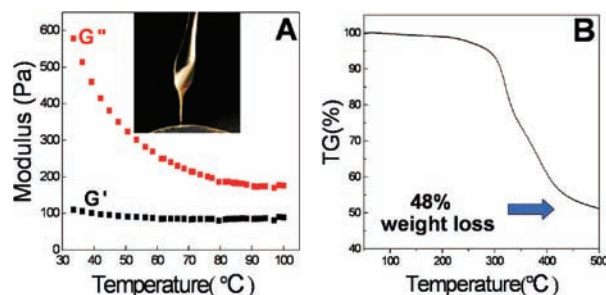


Figure 2. (A) Modulus–temperature trace and photo (inset) of CaCO₃ sulfonate nanosalt. (B) TGA trace of CaCO₃ sulfonate nanosalt.

copy (HRTEM) images showing clearly the core/shell structure of the functionalized CaCO₃ NPs, which confirmed the presumed structure of this family of functionalized NPs.

The rhombohedral CaCO₃ NPs can be seen from the transmission electron microscopy (TEM) image in Figure 1, and a two-step procedure of the functionalization is also presented. Surface modification of CaCO₃ NPs (20–50 nm size) through grafting a charged polysiloxane quaternary ammonium salt (DC5700) [(CH₃O)₃Si–(CH₂)₃N⁺(CH₃)₂(C₁₈H₃₇)Cl[–]] with an OH group renders the resulting nanoparticle cationic,¹⁸ which then reacts with sulfonate salts [C₉H₁₉–C₆H₄–O(CH₂CH₂O)₁₀SO₃[–]K⁺] through a cation–anion process to obtain the corresponding nanosalt.³

After purification, the cream-like CaCO₃ sulfonate nanosalt is obtained and exhibits obvious fluidity when it is slightly heated for a few seconds (Figure 2A, inset). The modulus–temperature trace (Figure 2A) also shows a liquid-like behavior considering that the shear loss modulus G'' of the CaCO₃ sulfonate nanosalt is higher than the storage modulus G' throughout the entire measured temperature range.^{3,6} As shown in thermogravimetric analysis (TGA) trace (Figure 2B), the CaCO₃ sulfonate nanosalt is solvent-free with an organic content of 48 wt % calculated from the weight

[†] School of Materials Science and Engineering.

[‡] State Key Laboratory of Advanced Technology for Materials Synthesis and Processing.

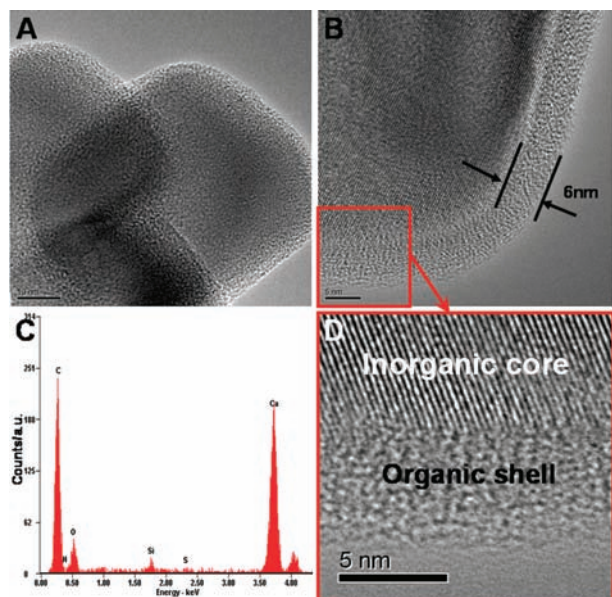


Figure 3. (A, B, and D) High-resolution TEM images of CaCO₃ sulfonate nanosalt at different magnifications. (C) EDX spectrum of CaCO₃ sulfonate nanosalt in (A).

loss, and a further calculation indicates that the organic phase possesses a volume fraction of 71% in this organic–inorganic hybrid nanosystem, which is high enough for it to act as the continuous phase and thus warrants fluidity.

Fourier transform infrared (FTIR) spectroscopy and XPS are applied to verify the surface functionalization (Figure S2, S3). The results show that both the modification of calcium carbonate NPs by DC5700 and the ionic exchange by the sulfonate ion are confirmed. The crystal structures of the original CaCO₃ NPs and the CaCO₃ sulfonate nanosalt are characterized by X-ray diffraction (XRD). Diffraction peaks of CaCO₃ with a calcite structure exist both before and after the surface functionalization (Figure S4), indicating that the crystal structure of CaCO₃ NPs remains unchanged. The agglomeration of NPs is abated after the functionalization according to the comparison between the TEM images of original CaCO₃ NPs and the CaCO₃ sulfonate nanosalt (Figure S4), which demonstrates that the surface functionalization can effectively alter the agglomeration behavior of CaCO₃ NPs.

To further verify the existence of the organic shell and its presumed structure, HRTEM images at different magnifications (Figure 3A, B, and D) are investigated. We can see that every CaCO₃ nanoparticle is well coated individually by an organic shell (Figure 3A, scale bar: 10 nm), and this ensures the stabilization of particle dispersion as well as the fluidity of this nanosystem. For the shell thickness, the estimated value from HRTEM image (Figure 3B, scale bar: 5 nm) and the calculated value are 6 and 5.9 ± 0.4 nm⁵ respectively, which indicates that the bilayer structure is as what we have conceived in Figure 1. In addition, the ordered crystal lattice of CaCO₃ NPs is shown in the HRTEM image in Figure 3D, with an interplanar distance of ~ 2.988 Å (Figure S5), which corresponds to the (104) plane of calcite and proves the existence of the inorganic phase. The results of energy-dispersive X-ray analysis (EDX, Figure 3C) show the elements in this system and are in agreement with the results of FTIR, confirming the successful surface modification with DC5700 and the sulfonate salts. The HRTEM image in Figure 3D also reveals the essence of the especial rheological property of this hybrid nanostructure by presenting a clear division between the inorganic core and the organic shell, for the soft organic shell enables the solid inorganic core to move

smoothly and exhibit liquid-like behavior. Namely, the organic shell serves as the “solvent” that can neither volatilize nor migrate.

In contrast to unmodified CaCO₃ NPs, the CaCO₃ sulfonate nanosalt is conductive over a temperature range of 16–90 °C according to the temperature dependence of conductivity (Figure S6). Since the CaCO₃ fluids possess comparatively large counterions and show flowability at room temperature, the conductivity is probably due to the local ion segment motion. Although the value is not high, for example, 4.5×10^{-6} S cm⁻¹ at 16 °C and 4.8×10^{-5} S cm⁻¹ at 90 °C, the functionality of conductivity coupled with the fluidity of CaCO₃ NPs provides the possibility to plasticize and toughen plastic and make plastic antistatic simultaneously.

In summary, we have reported, for the first time, the solvent-free fluids based on rhombohedral NPs of inorganic salt. The surface functionalization brings a number of promising properties to CaCO₃ NPs, such as conductivity, fluidity, and improved processability, all of which make CaCO₃ NPs attractive as plasticizers with effects of toughening, reinforcement, and conducting. Furthermore, we have verified the presumed structure of this family of functionalized NPs by judging from the direct evidence of the HRTEM images. This may assist in obtaining a better understanding of the essence of the peculiar rheological property and pave the way for further research into the structure of the solvent-free nanofluids on the nanometer scale.

Acknowledgment. This work was supported by the National Natural Science Foundation of China (NSFC: 50572081, 50802068), the National Key Technology R&D Program of China (No. 2007BAE10B02). We thank Prof. Chou Fan for XPS measurements.

Supporting Information Available: Experimental preparations, XPS C1s and Ca2p core levels from CaCO₃ NPs both before and after adjusting the pH value, XPS O1s core level from DC5700-grafted CaCO₃ NPs, DC5700 oligomers and CaCO₃ NPs after adjusting the pH value. FTIR spectra, XRD profiles, and TEM images for original CaCO₃ nanoparticle and CaCO₃ sulfonate nanosalt, temperature dependence of conductivity for CaCO₃ sulfonate nanosalt. This material is available free of charge via the Internet at <http://pubs.acs.org>.

References

- (1) Ciprari, D.; Jacob, K.; Tannenbaum, R. *Macromolecules* **2006**, *39*, 6565–6573.
- (2) Xiong, C.; Lu, S.; Wang, D.; Dong, L.; Jiang, D. D.; Wang, Q. *Nanotechnology* **2005**, *16*, 1787–1792.
- (3) Warren, S. C.; Banholzer, M. J.; Slaughter, L. S.; Giannelis, E. P.; DiSalvo, F. J.; Wiesner, U. B. *J. Am. Chem. Soc.* **2006**, *128*, 12074–12075.
- (4) Rodriguez, R.; Herrera, R.; Archer, L. A.; Giannelis, E. P. *Adv. Mater.* **2008**, *20*, 4353–4358.
- (5) Lei, Y.; Xiong, C.; Dong, L.; Guo, H.; Su, X.; Yao, J.; You, Y.; Tian, D.; Shang, X. *Small* **2007**, *3*, 1889–1893.
- (6) Bourlinos, A. B.; Herrera, R.; Chalkias, N.; Jiang, D. D.; Zhang, Q.; Archer, L. A.; Giannelis, E. P. *Adv. Mater.* **2005**, *17*, 234–237.
- (7) Bourlinos, A. B.; Chowdhury, S. R.; Herrera, R.; Jiang, D. D.; Zhang, Q.; Archer, L. A.; Giannelis, E. P. *Adv. Funct. Mater.* **2005**, *15*, 1285–1290.
- (8) Bourlinos, A. B.; Georgakilas, V.; Tzitzios, V.; Boukos, N.; Herrera, R.; Giannelis, E. P. *Small* **2006**, *2*, 1188–1191.
- (9) Bourlinos, A. B.; Georgakilas, V.; Boukos, N.; Dallas, P.; Trapalis, C.; Giannelis, E. P. *Carbon* **2007**, *45*, 1583–1595.
- (10) Lei, Y.; Xiong, C.; Guo, H.; Yao, J.; Dong, L.; Su, X. *J. Am. Chem. Soc.* **2008**, *130*, 3256–3257.
- (11) Han, B. H.; Winnik, M. A.; Bourlinos, A. B.; Giannelis, E. P. *Chem. Mater.* **2005**, *17*, 4001–4009.
- (12) Bourlinos, A. B.; Chowdhury, S. R.; Jiang, D. D.; An, Y. U.; Zhang, Q.; Archer, L. A.; Giannelis, E. P. *Small* **2005**, *1*, 80–82.
- (13) Bourlinos, A. B.; Raman, K.; Herrera, R.; Zhang, Q.; Archer, L. A.; Giannelis, E. P. *J. Am. Chem. Soc.* **2004**, *126*, 15358–15359.
- (14) Bourlinos, A. B.; Chowdhury, S. R.; Jiang, D. D.; Zhang, Q. *J. Mater. Sci.* **2005**, *40*, 5095–5097.
- (15) Ishida, H.; Miller, J. D. *Macromolecules* **1984**, *17*, 1659–1666.
- (16) Al-Hosney, H. A.; Grassian, V. H. *J. Am. Chem. Soc.* **2004**, *126*, 8068–8069.
- (17) Chaimberg, M.; Cohen, Y. *J. Colloid Interface Sci.* **1990**, *134*, 576–579.
- (18) Pottier, A.; Cassignon, S.; Chanéac, C.; Villain, F.; Tronc, E.; Jolivet, J.-P. *J. Mater. Chem.* **2003**, *13*, 877–882.

JA902197V